Special Issue - Neuroscience

Magnetoencephalography Phantom Comparison and Validation: Hospital Universiti Sains Malaysia (HUSM) Requisite

Hazim Omar[1], Alwani Liyana Ahmad[1], Noburo Hayashi[2], Zamzuri Idris[3,4], Jafri Malin Abdullah[3,4]

Submitted: 20 Oct 2015
Accepted: 5 Nov 2015

[1] *Department of Neurosciences, Hospital Universiti Sains Malaysia, Jalan Hospital USM, 16150 Kubang Kerian, Kelantan, Malaysia*

[2] *Elekta K K Shibaura Renasite Tower 3-9-1 Shibaura, Minato-ku, Tokyo 108-0023 Japan*

[3] *Department of Neurosciences, School of Medical Sciences, Universiti Sains Malaysia, 16150 Kubang Kerian, Kelantan, Malaysia*

[4] *Center for Neuroscience Services & Research, Universiti Sains Malaysia, 16150 Kubang Kerian, Kelantan, Malaysia*

Abstract

Background: **Magnetoencephalography (MEG) has been extensively used to measure small-scale neuronal brain activity. Although it is widely acknowledged as a sensitive tool for deciphering brain activity and source localisation, the accuracy of the MEG system must be critically evaluated. Typically, on-site calibration with the provided phantom (*Local phantom*) is used. However, this method is still questionable due to the uncertainty that may originate from the phantom itself. Ideally, the validation of MEG data measurements would require cross-site comparability.**

Method: **A simple method of phantom testing was used twice in addition to a measurement taken with a calibrated reference phantom (*RefPhantom*) obtained from Elekta Oy of Helsinki, Finland. The comparisons of two main aspects were made in terms of the dipole moment (Qpp) and the difference in the dipole distance from the origin (d) after the tests of statistically equal means and variance were confirmed.**

Result: **The result of Qpp measurements for the *LocalPhantom* and *RefPhantom* were 978 (SD24) nAm and 988 (SD32) nAm, respectively, and were still optimally within the accepted range of 900 to 1100 nAm. Moreover, the shifted d results for the LocalPhantom and RefPhantom were 1.84 mm (SD 0.53) and 2.14 mm (SD 0.78), respectively, and these values were below the maximum acceptance range of within 5.0 mm of the nominal dipole location.**

Conclusion: **The local phantom seems to outperform the reference phantom as indicated by the small standard error of the former (SE 0.094) compared with the latter (SE 0.138). The result indicated that HUSM MEG system was in excellent working condition in terms of the dipole magnitude and localisation measurements as these values passed the acceptance limits criteria of the phantom test.**

Keywords: *magnetoencephalography, validation, phantom*

Introduction

Non-invasive techniques have become important brain mapping techniques in the study of brain function. In the last five decades, the non-invasive functional imaging technology has advanced in a wide range of modalities, including magnetoencephalography (MEG) and electroencephalography (EEG). MEG-recorded magnetic fields are produced by electrical activity within the brain and recorded outside the head, whereas EEG is based on the measurements of potential differences on the scalp that result from ohmic currents induced by electrical brain activity (1). Both modalities measure the electromagnetic signals produced by the electrical activity in the brain. However, MEG possess more advantages than EEG because the neuronal signals generated

in the cortex pass several layers of tissue with different electrical properties and complex geometries before they reach the scalp; thus, the electrical fields that are recorded at the scalp are distorted. These issues have a weaker influence on the magnetic fields because the tissues surrounding the brain exhibit a constant magnetic permeability (2). Nevertheless, each modality has its own advantages and disadvantages because no single method is best suited for all research or clinical purposes. For example, both MEG and EEG have a basic limitation in that the neuronal signals are only recorded from the scalp, which is less sensitive than recording from deep sources(3). The localisation of EEG and MEG source activities in the brain is discombobulated because there is an indefinite number of source configurations that could give rise to the same measurements. This problem is known as the inverse problem (4).

MEG and EEG are capable of detecting direct neural electrical currents and mapping functional brain activities at a temporal resolution as small as a fraction of a millisecond and a spatial resolution of several millimetres (5). The magnetic signals associated with bioelectrical activity are very weak; therefore, special techniques are needed to discriminate these signals from extraneous magnetic fields, i.e., noise. MEG systems involve an array of sensors that are divided into two types, i.e., magnetometers and gradiometers, and each type is coupled to a special, low-noise amplifier. MEG recording must be performed inside a magnetically shielded room to reduce extraneous magnetic fields (6). The primary source of electromagnetic signals is the current flow in the apical dendrites of pyramidal cells in the cerebral cortex. Because the columnar organisation of the cortex is oriented normal to its surface, the coherent activation of a small area results in a huge number of these pyramidal cells of the cortex being activated in a manner that can be modelled as an equivalent current dipole (ECD) (7). These current dipoles can typically be found within the cortical grey matter, and they are the basic element used to represent neural activation in MEG- and EEG-based inverse methods (1).

ECDs and clusters of such dipoles are used to represent focal neural activity. The modelled ECD information is particularly frequently used to estimate of the locations and amplitudes of the equivalent dipoles via the inverse procedure. These sources can be estimated accurately by performing MEG recoding when the true locations and temporal activities of the dipoles are known (8). To achieve this aim, artificial objects that mimic human brain activity called "phantoms" are constructed by the manufacturers of MEG systems and used to evaluate the accuracies of MEG measurements. Such phantoms are normally delivered in the package with the MEG system and intended for local and daily maintenance of the system at the site to ensure verification of the MEG measurements. The most common use of such provided phantoms is to pass electric current through electrodes with pre-determined locations inside the phantom. The estimated locations of the ECDs as measured by the MEG system via inverse method calculations are then compared to the pre-determined "true position" of the signal origin based on the structure of the phantom. The divergence between the projected dipole position and the origin of the electrode or the "true position" is considered as an evaluation of the accuracy of the MEG system (9). Nonetheless, this method is questionable because the uncertainty of the measurement may not lie within the MEG system but within phantom itself (Local Phantom).

To confirm the reliability and traceability of local phantom measurements and the efficiency of the HUSM MEG system, a reference phantom specifically designed by Elekta Oy was used. This reference phantom possessed shape and dipole structures that were identical to those of the local phantom and was used in multiple MEG system sites as a reference. Hence, comparison of the data uncertainties and dispersions from the two phantoms is a reasonable method for the evaluation of the data accuracy when the reference phantom has been conditionally calibrated, and this approach can thus ensure confidence in the assessments (10).

Therefore, the objectives of this experiment were to compare the accuracies of the local and reference phantoms and to demonstrate that HUSM MEG system measurements were valid and fell within the acceptance limits.

Materials and Methods

Phantom

The system performance was examined using the provided phantom, which contains 32 simulated dipoles and four pre-set head position indicator (HPI) coils. The hemispheric shape of the phantom was designed to create equivalent magnetic field distributions based on assembled equilateral triangular line currents that generate tangential current dipoles inside the sphere. This arrangement provisionally created such that the vertex of the triangle and the origin of the conducting sphere coincide. The currents are then fed through an inbuilt generator to excite

the artificial dipoles via a dipole multiplexer. The dipoles are activated sequentially up to 32 times to generate typical evoked responses that are then analysed for accuracy.

Two designated phantoms were used in the validation procedure, i.e., a local phantom (LocalPhantom) that was supplied with the MEG system and a reference NM24058N phantom (serial number: 101861; RefPhantom) provided by Elekta Oy of Helsinki Finland that had been calibrated by the Department of Mechanical Engineering and Industrial Systems of the Tampere University of Technology (Figure 1).

Methods

The phantom tests were performed as instructed in the Elekta Neuromag Data Acquisition User's Manual NM23065A-A (11).

The phantom was connected to an excitation multiplexer attached to 25-pin socket connector located under the side cover of the gantry. After loading the built-in measurement setting parameters located in the file /neuro/dacq/setup/phantom.fif, the acquisition programme proceeded with the digitisation of the HPI coil (Figure 2). These cardinal points were verified to coincide with the HPI coil before the phantom was placed in the probe unit of the gantry helmet. The set up was carefully arranged such that the front coil pointed upward, and the 32-pair cable and HPI coil were fit into the respective outlets under gantry side cover (Figure 3). Later, the dipole utility programme was executed, which involved the activation of the first dipole, and the display of the raw sine signal and the trigger. Subsequently, the average option button was clicked to record the average of 100 epochs for a single dipole. The current version of the HUSM MEG software allows for the continuous recording of a total of 32 dipoles without the need to manually reset the channel for each dipole.

The measurement file was created automatically when the recording was completed. Source modelling software was used to analyse the dipole fitting in which the setting for the sphere of origin was (0,0,0) in the head coordinate system, and the baseline was set from -50 to 0 ms. The localisation result was compared with the nominal data provided by the MEG system. Two main aspects of the comparison were examined; i.e., the amplitude of the dipole (Qpp) should be within the range of 900 nAm to 1100 nAm, and the displacement (mm) of the dipole from the nominal location (d) should not have exceeded 5 mm. The measurement of the dipole was then repeated using the other phantom (RefPhantom). These two measurements were then examined to gain insight into the correlation and validity of the comparison using a simple unpaired t test after the normality of the data distribution has been confirmed visually (Figure 4) and statistically.

Figure 1: Reference phantom (RefPhantom) NM24058N (Serial number: 101861) provided by Elekta Oy, Helsinki Finland. 32 built in simulated dipoles and four presetting head position indicator coils (HPI).

Results

The full results of dipole moment magnitude (Qpp) and difference in distance from the origin of the phantom are reported in Table 1a while the normality test results of skewness and kurtosis are displayed in Table 1b. Later the Z-score can be calculated in determining the type of data distribution. The Z-scores of the skewness and kurtosis tests that fell within the range of -1.19 to +1.96 indicated that the data were normally distributed (12,13).

Additionally, as demonstrated in Figure 5, the dots that appeared along the line in the q-q plot indicated that the observed data were approximately normally distributed.

A normality test conducted with SPSS was applied to acquire information about the distribution of the data. The distribution characteristics were determined based on

Figure 2: The digitisation of the phantom including the head positioning indicator (HPI) coil (4 point).

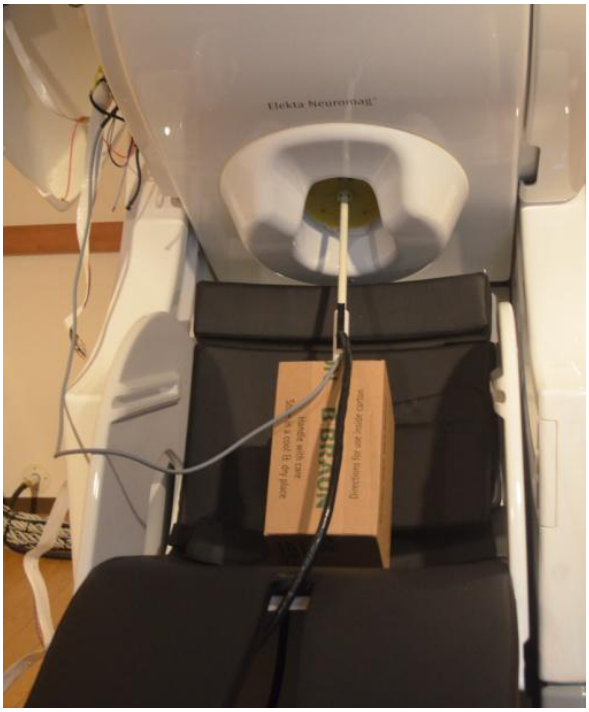

Figure 3: Phantom is carefully set into sensor helmet of the probe unit and pushed again helmet. HPI coil is fitted into outlet under right gantry side cover.

the skewness and kurtosis test scores, which indicated approximately normal distributions of all of the data sets. Based on the phantom dipole moment (Qpp) skewness scores of -0.122 (SE = 0.414) and 0.41 (SE = 0.414) and kurtosis scores of -0.201 (SE = 0.809) and 0.161 (SE = 0.809) for the local phantom and the reference phantom, respectively, the values were considered small and close to zero. To statistically quantify how far the skewness and kurtosis departed from their standard errors (SEs), the Z-values were calculated by dividing the skewness and kurtosis scores by the respective standard errors (SE).

The same approach was applied to the difference in the dipole distance (d) from the nominal location of the phantom. The differences in the dipole distance for the local phantom (dloc) and the reference phantom (dref) were -0.022 (SE = 0.414) and -0.723 (SE = 0.414), respectively, in the skewness tests, and scores of -0.220 (SE = 0.809) and 0.122 (SE = 0.809), respectively, were observed in the kurtosis test (Table 1b).

Discussion

All of the data for both the local and reference phantoms were slightly skewed and kurtotic, but they did not significantly differ from normal. We thus assumed that our data were approximately normally distributed in terms of skewness and kurtosis. The Z-scores for the skewness and Kurtosis tests fell in the range of -1.19 to +1.96, which indicated that the data were normally distributed (12,13).

Visual inspection of the histograms further indicated that all the data sets approximated the shape of a normal curve. The Q-Q plots of the data also provided evidence of normal distributions because the series of dot indicators fell along the line.

It is important to demonstrate that the dependent variable data are approximately normally distributed for each category so that the appropriate test can be used for the comparison. Unpaired or independent parametric t tests were used to explore and investigate the relationships of the data sets.

A t test between the local phantom and reference phantom was an appropriate approach to affirming that the measurements of the dipole moment (Qpp) and dipole localization were valid because both phantoms had the same design, which contained 32 artificial dipoles. A Levene's test yielded a F (62) = 1.784 and P = 0.187, which indicated that the variances of both phantoms were approximately equal (Table 2a, b). Thus, the

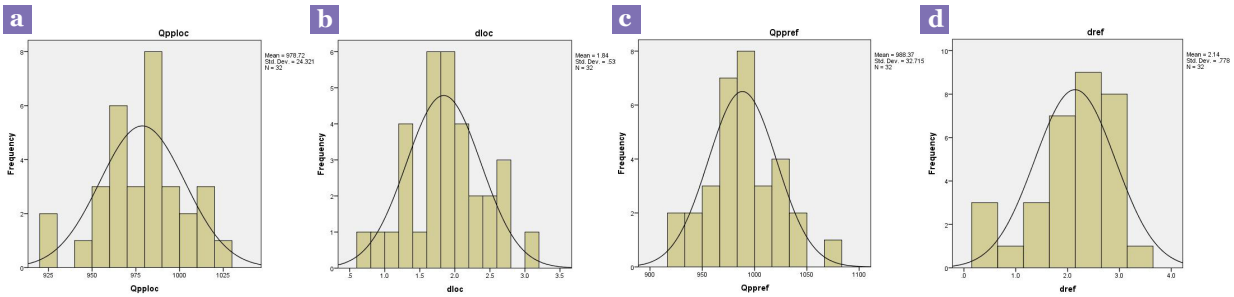

Figure 4: (a) The histogram of 32 dipole moment (Qpploc) for local phantom with mean 978.72 nAm, std dev. 24.32 nAm overlaid with normal distribution curve. (b) The histogram of 32 dipole difference in distance from nominal location (dloc) for local phantom with mean 1.84 m, std dev. 0.53 m overlaid with normal distribution curve. (c) The histogram of 32 dipole moment (Qppref) for reference phantom with mean 988.38 nAm, std dev. 32.72 nAm overlaid with normal distribution curve. (d) The histogram of 32 dipole difference in distance from nominal location (dref) for reference phantom with mean 2.14 m, std dev. 0.78 m overlaid with normal distribution curve.

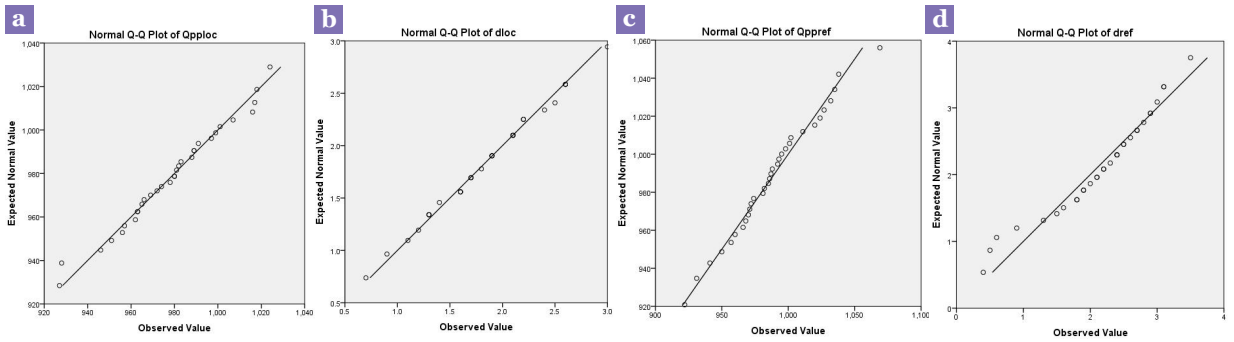

Figure 5: (a) The quantile-quantile (Q-Q) plot of 32 dipole moment (Qpploc) for local phantom overlaid with normal distribution line. (b) The quantile-quantile (Q-Q) plot of 32 dipole difference in distance from nominal location (dloc) for local phantom overlaid with normal distribution line. (c) The quantile-quantile (Q-Q) plot of 32 dipole moment (Qppref) for reference phantom overlaid with normal distribution line. (d) The quantile-quantile (Q-Q) plot of 32 dipole difference in distance from nominal location (dref) for reference phantom overlaid with normal distribution line.

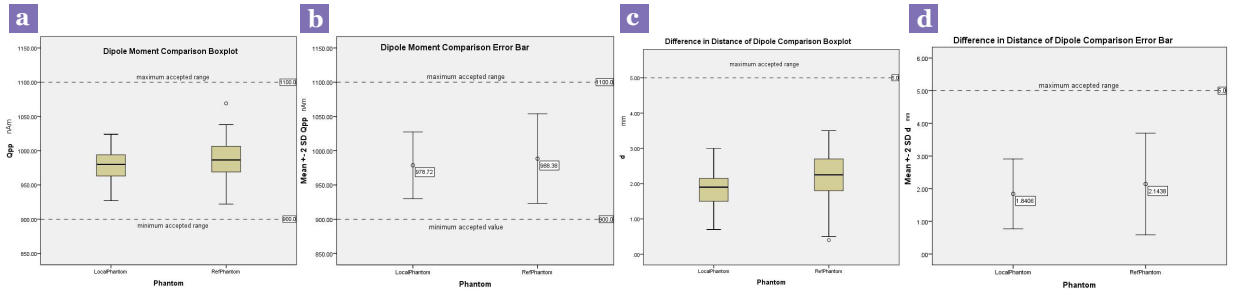

Figure 6: (a) The box plot of dipole moment (Qpp) for both local phantom and reference phantom illustrated all the datas including the outlier are still within permitted range of 900 nAm to 1100 nAm. (b) The error bar of dipole moment (Qpp) for both local phantom and reference phantom illustrated the extensively overlapping error bar which means no significant difference in data values. All the data values are still within permit able range. (c) The box plot of dipole difference in distance from nominal location (d) for local and reference phantom illustrated all the datas including the outlier are still under permitted value (5 mm). (d) The error bar comparison of dipole difference in distance from nominal location (d) for local and reference phantom shoed the extensively overlapping error bar which means no significant difference in data values. All the data values are still below maximum accepted range.

Table 1a: The test result of 32 dipole measurement for both phantoms

Dipole	*Qpploc (nAm)*	*dloc (m)*	*Qppref (nAm)*	*dref (m)*
1	980	1.6	1038	2.4
2	983	1.3	1020	2.1
3	965	1.3	998	1.8
4	974	1.2	1069	3.1
5	997	2.4	1002	2.6
6	956	1.9	993	2.5
7	1001	1.9	1011	2.1
8	1018	2.1	1035	3.1
9	946	2.2	966	2.4
10	966	1.7	950	2.8
11	962	1.3	1027	3.5
12	978	0.7	941	1.9
13	989	2.1	995	2.7
14	972	1.9	981	1.8
15	969	2.1	988	1.6
16	963	1.8	992	1.3
17	999	1.9	985	2
18	957	1.6	960	2.2
19	951	1.4	931	2.3
20	928	2.2	922	2.9
21	989	2.5	987	2.5
22	982	2.6	986	2.4
23	981	1.7	972	2.9
24	980	2.1	957	2.7
25	1016	2.6	1024	2.2
26	1007	1.9	982	0.9
27	963	1.1	968	0.5
28	991	1.6	971	0.6
29	1017	3	1032	3
30	1024	2.6	1001	1.9
31	988	1.7	970	1.5
32	927	0.9	974	0.4
Average	978.72	1.84	988.38	2.14

The test result of 32 dipole moment magnitude (nAm) for local phantom (Qpploc) and reference phantom (Qppref) as well as the result for difference in distance from origin (m) of local phantom (dloc) and reference phantom (dref).

standard t test results were used. The result of the independent t test was not significant (t (62) = -1.34, P = 0.185), which indicated that there was no significant difference between the phantoms. The 95% confidence interval of the difference between the means was -24.06 to 4.75.

Similarly, the test was applied to the differences in the dipole distances from the phantom origins (d) for both phantoms. A Levene's test revealed that the difference in distance (d) had an equal variance as indicated by an F (62) = 3.141 and P = 0.081, which indicated a non-significant result (Table 2 c,d). Hence, the standard t test was used and yielded the score of t(62)=-1.818, p=0.074, which indicated that there was no significant difference in the mean (d) between the both phantoms. The 95% confidence interval of the difference was -0.63 to 0.03.

Based on these test results, it can be assumed that both phantoms were similar in dipole magnitude and dipole location characteristics. Consequently, the comparisons of the accuracies of the dipole magnitude and dipole location were verified.

Accordingly, the test results were then compared to the accepted limits for the phantom test. If the test result falls within the accepted value range, the local phantom (LocalPhantom) and the MEG system meet the national standard in Europe. The dipole moments (Qpps) for the LocalPhantom and RefPhantom were 978 (SD 24) nAm and 988 (SD 32) nAm, respectively. Although there was an outlier in the RefPhantom as indicated in the dipole moment comparison boxplot, all of the dipoles magnitudes were still within the accepted range of 900 to 1100 nAm. The same pattern can be observed in the dipole moment comparison error bar. Impressively, the LocalPhantom exhibited an accuracy and precision that were superior to those of the RefPhantom in terms of the dipole magnitude. This finding is illustrated by the observation that the dipole moment comparison standard error of the LocalPhantom was distinctly smaller (SE 4.299) than that of the RefPhantom (SE 5.783).

Correspondingly, the differences in the dipole distances from the origin (d) for the LocalPhantom and the RefPhantom were 1.84 (SD 0.53) mm and 2.14 (SD 0.78) mm, respectively. Again, there was an outlier in the RefPhantom data regarding the difference in the distance of the comparison boxplot. However, the outlier and the rest of the data (d) were still below the maximum acceptable range, which was within 5.0 mm of the nominal dipole location. The error bar for the distance from the nominal dipole (d) was

Table 1b: The normality test result of the phantoms

	N	Minimum	Maximum	Mean	SD	Skewness			Kurtosis		
	Statistic	Statistic	Statistic	Statistic	Statistic	Statistic	Std. Error	Z-score	Statistic	Std. Error	Z-score
Qpploc	32	927	1024	978.72	24.321	-0.122	0.414	-0.295	-0.163	0.809	-.201
dloc	32	0.7	3.0	1.841	0.5333	-0.022	0.414	-0.053	-0.220	0.809	-.271
Qppref	32	922	1069	988.38	32.715	0.241	0.414	0.582	0.161	0.809	.199
dref	32	0.4	3.5	2.144	0.7779	-0.723	0.414	-1.743	0.122	0.809	.151

The normality test result of respective dipole moment magnitude (Qpp) (nAm) and the difference in distance from origin (d) (m) for local phantom (loc) and reference phantom (ref).

Table 2a: The general statistic test result of dipole moment magnitude (Qpp)

	Phantom	N	Mean	SD	SEM
Qpp	LocalPhantom	32	978.7188	24.32075	4.29934
	RefPhantom	32	988.3750	32.71455	5.78317

The statistic test result of dipole moment magnitude (Qpp) (nAm) for local phantom (loc) and reference phantom (ref).

Table 2b: The *t* test result of dipole moment magnitude (Qpp) (nAm) of the phantoms

		Independent Samples Test								
		Levene's Test for Equality of Variances		t-test for Equality of Means					95% Confidence Interval of the Difference	
		F	Sig.	t	df	Sig. (2-tailed)	Mean Difference	Std. Error Difference	Lower	Upper
Qpp	Equal variances assumed	1.784	0.187	-1.340	62	0.185	-9.65625	7.20621	-24.06125	4.74875
	Equal variances not assumed			-1.340	57.248	0.186	-9.65625	7.20621	-24.08507	4.77257

The *t* test result of dipole moment magnitude (Qpp) (nAm) for local phantom (loc) and reference phantom (ref) demonstrated that Levene's significant score 0.187 which is higher than $P = 0.05$. This means that both dipole phantom data is having the equal variance.

Table 2c: The general statistic test result of dipole difference in distance from origin (d) (m) of the phantoms

	Group Statistics				
	Phantom	N	Mean	Std. Deviation	Std. Error Mean
d	LocalPhantom	32	1.8406	0.53332	0.09428
	RefPhantom	32	2.1438	0.77790	0.13751

General statistic test result of dipole difference in distance from origin (d) (m) for local phantom (loc) and reference phantom (ref).

Table 2d: *t* test result of dipole difference in distance from origin (d) (m) of the phantoms.

		Independent Samples Test								
		Levene's Test for Equality of Variances		t-test for Equality of Means					95% Confidence Interval of the Difference	
		F	Sig.	t	df	Sig. (2-tailed)	Mean Difference	Std. Error Difference	Lower	Upper
d	Equal variances assumed	3.141	0.081	-1.818	62	0.074	-0.30312	0.16673	-0.63641	0.03016
	Equal variances not assumed			-1.818	54.869	0.075	-0.30312	0.16673	-0.63727	0.03102

The *t* test result of dipole difference in distance from origin (d) (m)for local phantom (loc) and reference phantom (ref) demonstrated that Levene's significant score 0.081 which is higher than $P = 0.05$. This means that both dipole phantom data is having the equal variance.

narrower for the LocalPhantom (SE 0.094) than the RefPhantom (SE 0.138), which again indicated that the LocalPhantom performed better than the RefPhantom.

Conclusion

The local phantom measurements were validated by demonstrating that the collected data were comparable to those of the reference phantom in terms of the statistically equivalent means and variances; thus, the HUSM MEG system measurements were validated as being within the acceptable limits of the phantom test. Therefore, this system was assumed to be in excellent working condition in terms of dipole magnitude and dipole localisation measurements. The measurements from this HUSM MEG system were acceptable according to the national standard in Europe.

Acknowledgement

The authors would like to thank Jukka Knuutila of the Elekta Oy, Helsinki, for assistance with the designing and calibration of the reference phantom. This research was supported by Hospital Universiti Sains Malaysia in ensuring the optimal diagnostic services to the patients and research.

Funds

None.

Conflicts of Interests

None.

Authors' Contributions

Conception and design: HO, ALA, ZI, JMA
Analysis and interpretation of the data: HO, ALA, NH
Drafting of the article: HO, ALA
Critical revision of the article for important intellectual content: ALA, ZI, JMA
Final approval of the article ZI, JMA
Provision of study materials or patients: NH
Statistical expertise, administrative, technical, or logistic support, collection and assembly of data: HO, NH

Correspondence

Mr Hazim Omar
BASc Medical Physics (USM), MSc Translational Neuroimaging (University of Nottingham)
Department of Neurosciences
Hospital Universiti Sains Malaysia
Universiti Sains Malaysia
16150 Kubang Kerian
Kelantan, Malaysia
Tel: +609-767 4046
Fax: +609-767 3833
Email: hazim@usm.my

References

1. Darvas F, Pantazis D, Yildirim E, Leahy RM. Mapping human brain function with MEG and EEG: methods and validation. *Neuroimage*. 2004;**23 (Suppl 1)**: S289–299. doi: 10.1016/j.neuroimage.2004.07.014.

2. Fernando Lopes da silva. EEG and MEG: Relevance to Neuroscience. *Neuron*. 2013;**80(5)**:1112–1128. doi: 0.1016/j.neuron.2013.10.017.

3. Hansen PC, Kringelbach ML, Salmelin R. *MEG : an introduction to methods*. New York (NY): Oxford University Press. xii. 2010. p. 436.

4. Hämäläinen M, Hari R, Ilmoniemi RJ, Knuutila J, Lounasmaa OV. Magnetoencephalography-theory, instrumentation, and applications to noninvasive studies of the working human brain. *Rev Mod Phys*. 1993;**65(2)**:413–497. doi: 10.1103/RevModPhys.65.413.

5. Sung CJ. MEG and EEG fusion in Bayesian frame. *Electronics and Information Engineering (ICEIE)*. 2010;**2**:295–299. doi: 10.1109/ICEIE.2010.5559785.

6. Papanicolaou A, Eduardo MC, Billingsley-Mashall R, Pataraia E. Simos PG. A review of clinical applications of magnetoencephalography. *Int Rev Neurobiol*. 2005;**68**:223–247. doi: 10.1016/S0074-7742(05)68009-9.

7. Okada YC, Wu J, Kyuhou S. Genesis of MEG signals in a mammalian CNS structure. Electroencephalogr. *Clin Neurophysiol*. 1997;**103(4)**:474–485. doi: 10.1016/S0013-4694(97)00043-6.

8. Leahy RM, Mosher JC, Spencer M, Huang MX, Lewine JD. A study of dipole localization accuracy for MEG and EEG using a human skull phantom. Electroencephalogr. *Clin Neurophysiol*. 1998;**107(2)**:159–173. doi: 10.1016/S0013-4694(98)00057-1.

9. Oyama D. Dry phantom for magnetoencephalography -Configuration, calibration, and contribution. *J Neurosci Methods*. 2015;**251**:24–36. doi: 0.1016/j.jneumeth.2015.05.004.

10. Metrology BJCfGi. *Evaluation of measurement data – Guide to the expression of uncertainty in measurement JCGM 100:2008, in (GUM 1995 with minor corrections)*. Paris; 2008:JCGM 100:2008:

11. Oy EN. *Magnetoencephalography Data Acquisition User's Manual*. Helsinki, Finland; Elekta: 2007.

12. Kim HY. Statistical notes for clinical researchers: assessing normal distribution (2) using skewness and kurtosis. *Restor Dent Endod*. 2013;**38(1)**:52–54. doi:10.5395/rde.2013.38.1.52.

13. Cramer D. F*undamental statistics for social research: step-by-step calculations and computer techniques using SPSS for Windows*. London [England], New York; Routledge. 1998. p. 456.